Very Long Baseline Interferometry Using a Radio Telescope in Earth Orbit

J. S. Ulvestad, C. D. Edwards, and R. P. Linfield
Tracking Systems and Applications Section

Successful Very Long Baseline Interferometry (VLBI) observations at 2.3 GHz have been made using an antenna aboard an earth-orbiting spacecraft as one of the receiving telescopes. These observations employed the first deployed satellite (TDRSE-E for East) of the NASA Tracking and Data Relay Satellite System (TDRSS). Fringes were found for 3 radio sources on baselines between TDRSE and telescopes in Australia and Japan. This article describes the purpose of the experiment and the characteristics of the spacecraft that are related to the VLBI observations. It goes on to explore the technical obstacles to maintaining phase coherence between the orbiting antenna and the ground stations, as well as the calibration schemes for the communications link between TDRSE and its ground station at White Sands, New Mexico. System coherence results and scientific results for the radio source observations are presented. Using all available calibrations, a coherence of 84% over 700 seconds was achieved for baselines to the orbiting telescope.

I. Introduction

Very Long Baseline Interferometry (VLBI) is a technique that uses the correlation of data recorded at two or more separate telescopes in order to achieve high angular resolution. For ground-based VLBI, the maximum projected baseline and consequent resolution are limited by the physical diameter of the earth. It has been proposed that a spacecraft dedicated to VLBI be launched so that the orbiting observatory could be used for improved resolution and mapping of compact radio sources. The two major projects currently being studied are the QUASAT project, involving NASA and the European Space Agency, and the RADIOASTRON project under way in the Soviet Union. Reference 1 describes various space VLBI concepts and the scientific benefits of doing VLBI from space. More up-to-date status reports on QUASAT and RADIOASTRON are given in Refs. 2 and 3.

Several technical hurdles must be cleared in order to use a free-flying spacecraft as a VLBI telescope. First, a local oscillator purity of 10^{-13}-10^{-12} is needed on board the spacecraft. This might be achieved either by having an accurate oscillator in space or by successfully transferring a frequency reference from the ground to the spacecraft via a communications uplink. Second, the spacecraft orbit must be adequately known, and variations in that orbit modelled or calibrated accurately enough to permit lengthy coherence times. Third, the wide-band VLBI data must be transmitted to the ground and recorded there. A demonstration that these problems

could be solved in a VLBI experiment using an element of TDRSS was proposed several years ago (Ref. 4) and carried out in July and August of 1986. A secondary purpose of such an experiment was the investigation of compact extragalactic radio sources on baselines longer than the earth's diameter and the demonstration that a dedicated VLBI observatory in space could accomplish scientifically valuable goals. This article describes the results of the successful space VLBI experiment carried out in 1986. The primary results of the experiment were first reported in Ref. 5.

II. Design of an Experiment Using TDRSE

The TDRSE satellite is in geosynchronous orbit at 41° west longitude, above the western part of the Atlantic Ocean. It has two 4.9 m antennas that operate near 2 GHz (S-band) and 15 GHz (K-band). In addition, there is a smaller antenna that is used for the uplink (15 GHz) and downlink (14 GHz) to the ground control station at White Sands, New Mexico. Each 4.9 m antenna has a 3 dB bandwidth of 16 MHz and a system temperature of approximately 320 K (see Ref. 5 for more details of the antenna calibration). The two 4.9 m antennas have separate intermediate frequency chains that are driven by a common local oscillator on the spacecraft; that oscillator is tied to a cesium frequency standard at White Sands which is transferred to the spacecraft via the 15 GHz uplink. Orbit determination for TDRSE is normally done using range and Doppler data acquired with two widely spaced ground transponders in the Bilateration Ranging Transponder System (BRTS).

The TDRSS system is designed primarily to track and relay communications from satellites in low earth orbit. The normally allowed pointing window for a 4.9 m antenna on the spacecraft is a square 28° on a side, centered at the nadir. This is adequate for covering satellites near the earth, which has an angular radius of about 9° as viewed from geosynchronous orbit. In fact, our observations were further limited by the restriction that we were only allowed to observe sources at southern declinations. A pointing window consisting of the southern half of an ellipse with a semi-major axis of 31° (north-south) and a semi-minor axis of 23° (east-west) was supposed to be available for the VLBI experiment. However, problems with the software used to point the spacecraft antennas prevented us from making any successful observations outside the southern half of the 28° square. Figure 1 displays the field of view of a TDRSE antenna.

The low sensitivity of the spacecraft antenna and the pointing limits restricted the choice of ground antennas that could be used in the orbiting VLBI (OVLBI) experiment. Specifically, very sensitive telescopes on the side of the earth opposite TDRSE were required. Therefore, the observations were made using the 64 m antenna of the NASA Deep Space Station at Tidbinbilla, Australia; and the 64 m antenna of the Japanese Institute for Space and Astronautical Science (ISAS), at Usuda, Japan. In addition, the 26 m antenna of the Radio Research Laboratory (RRL) at Kashima, Japan was used during most of the OVLBI observations in order to check the performance of the larger ground antennas. After an S-band maser receiver from the Jet Propulsion Laboratory was installed on the telescope at Usuda, both 64 m telescopes had system temperatures of about 15-20 K.

The low spacecraft sensitivity also meant that it was necessary to use the widest feasible bandwidth and the longest possible integrations in the VLBI observations. The large bandwidth was achieved by using the Mark III VLBI recording system (Ref. 6) in Mode E. Seven contiguous 2 MHz channels centered at 2277.99 MHz were recorded, giving a total bandwidth of 14 MHz. This is nearly the maximum bandwidth available from TDRSE. The data from the celestial radio sources were recorded directly in the usual way at Usuda and Tidbinbilla. The wide-band data received by TDRSE were coherently translated to the downlink frequency of 14 GHz, transmitted to the ground, translated to an intermediate frequency of 370 MHz, and fed directly into the video converters of the Mark III recorder. Details of the methods used to achieve the greatest possible system coherence (hence, the longest possible integration times) are given in Section III below.

III. Coherence and Stability

A. Coherence Requirements for Interferometry

The coherence for an integration time T can be defined:

$$C(T) = \left\| \frac{1}{T} \int_0^T dt\, e^{i\tilde{\phi}(t)} \right\|$$

where $\tilde{\phi}$ is the residual interferometer phase after removal of a linear trend (Ref. 7). For $\tilde{\phi}(t) \ll 1$ radian, $C(T) \approx 1$; as the phase residuals grow to an order of 1 radian or more, the coherence drops off quickly. Since the observed fringe amplitude is proportional to the coherence, $C(T)$ can be thought of as an efficiency factor.

Based on this dependence of the coherence on the rms phase fluctuations, one can formulate a rough stability requirement for maintaining coherence. For an integration time of length τ at an observation frequency ν_{RF}, the Allan (or two-point) variance $\sigma_y(\tau)$ must satisfy:

$$\nu_{RF}\, \tau\, \sigma_y(\tau) < 1 \text{ radian}$$

The minimum value of τ is given by signal-to-noise considerations. To have a high probability of fringe detection on the baseline between a TDRSE 4.9 m antenna and either of the 64 m ground antennas, it was necessary to ensure good coherence out to 500 s. Given an observing frequency of 2.3 GHz, this translates to a stability requirement of $\sigma_y(\tau) < 1 \times 10^{-12}$.

B. Contributions to Phase Instability of the Experiment

Some of the sources of phase instability for the OVLBI experiment were typical of any VLBI experiment; others were a direct consequence of using an orbiting antenna. First consider spacecraft-specific error sources. The most important consideration here is the effect of spacecraft motion. Changes in the spacecraft position change the geometric delay between TDRSE and the ground stations. The observation frequency of 2.3 GHz corresponds to a wavelength of about 13 cm. Thus a 13 cm change in spacecraft position (in the direction of the observed quasar) would change the geometric phase by a full cycle. Even more important, however, is the effect of spacecraft motion on the communications link between TDRSE and the White Sands ground station. The local oscillators onboard TDRSE are derived from a 15 GHz pilot tone uplink from White Sands, while the observed signal is transmitted back to White Sands on a 14 GHz downlink. After accounting for frequency translation onboard the spacecraft, the relevant frequency at which spacecraft position errors affect the TDRSE-White Sands communications link is roughly twice the downlink frequency, or more than 25 GHz, which corresponds to an effective wavelength of about 1 cm. Namely, a 1 cm change in the line-of-sight distance between TDRSE and White Sands will result in nearly a full cycle phase shift of the signal recorded at White Sands. To maintain good coherence for integration times of 500 s, it follows that TDRSE accelerations must be modeled or calibrated to better than 10^{-8} m/s^2.

Other error sources are more typical of ground-based observations. Independent frequency standards are used at each site to generate local oscillators and to time tag the recorded data. A hydrogen maser, with $\sigma_y(\tau = 500\text{ s}) < 1 \times 10^{-14}$, was used at the DSN 64 m station in Australia. Usuda used a rubidium standard, with $\sigma_y(\tau = 500\text{ s}) \approx 2 \times 10^{-13}$. At White Sands, a cesium standard with stability $\sigma_y(\tau = 500\text{ s}) \approx 4 \times 10^{-13}$ was used as the frequency reference for all the TDRSS local oscillators, both or the ground and onboard the spacecraft, via the uplink pilot tone. A hydrogen maser was used, however, to drive the Mark III terminal equipment at White Sands.

Propagation media effects also contribute to phase instability. The troposphere will affect the 2.3 GHz observations at the ground antennas, but more important in terms of phase stability is its effect on the higher frequency TDRSE-White Sands links. For the ionosphere the situation is reversed, as the phase effect of the ionosphere scales as $1/\nu$. The ionosphere should not be a factor for the uplink and downlink to TDRSE, due to the high link frequencies, but will be important at the 2.3 GHz observation frequency.

Finally, instrumental instabilities must be considered. Of particular concern is the stability of the TDRSE spacecraft instrumentation. This includes both the physical stability of the 4.9 m antennas and the stability of the various RF receivers, mixers, and local oscillators.

C. December 1985 Stability Test Results

To determine the suitability of TDRSS for OVLBI, tests were performed at White Sands in December, 1985. In one configuration, a 2.3 GHz beacon at White Sands was observed by one of the 4.9 m TDRSE antennas and transferred back to White Sands, where the tone was tracked and phase residuals recorded. Later, the TDRSE ephemeris based on BRTS data (standard range and doppler measurements) was used to remove the effects of spacecraft motion. Phase fluctuations of roughly $\pm 1/4$ cycle remained, with coherence falling quickly from 95% at 100 s to less than 60% at 500 s.

To improve coherence, a second test was performed in which both 4.9 m antennas observed the ground beacon. Phase residuals observed in one channel were used to correct the phase in the other channel, thereby calibrating all effects on the TDRSE-White Sands link common to both channels, including propagation media, common spacecraft instrumental instabilities, spacecraft motion, and instabilities in the ground frequency standard. In this configuration, the phases observed in the two channels tracked each other to about ± 0.02 cycles, yielding a relative coherence of better than 99% for 1000 s.

D. TDRSE Ephemeris Calibrations

Based on the December stability tests, it was decided that the astronomical observations would employ one TDRSE 4.9 m antenna to track a 2.3 GHz ground beacon while the other 4.9 m antenna observed an extragalactic radio source. This setup provided two sources of information on spacecraft position: the BRTS data and the tracked beacon phase. The BRTS data provided a full three-dimensional spacecraft ephemeris, while the beacon data yielded more accurate information, but only along the TDRSE-White Sands line-of-sight. Figure 2 depicts the configuration used for the quasar observations, while Fig. 3 is a simplified block diagram of the overall system.

During correlation at Haystack Observatory, delay and phase models must be supplied which account for the effects

of TDRSE motion. The model interferometer delay for the baseline between TDRSE and Usuda (for example) is given by:

$$c\tau = [\vec{r}_{\mathrm{USUDA}} - \vec{r}_{\mathrm{TDRSE}}] \cdot \hat{\epsilon}_{\mathrm{QSO}} + \|\vec{r}_{\mathrm{WS}} - \vec{r}_{\mathrm{TDRSE}}\|$$

where $\vec{r}_{\mathrm{TDRSE}}$ and $\vec{r}_{\mathrm{USUDA}}$ are the position vectors for TDRSE and Usuda, $\vec{r}_{\mathrm{WS}}$ is the position vector for the White Sands ground station, and $\hat{\epsilon}_{\mathrm{QSO}}$ is a unit vector in the quasar direction. This delay is a sum of two terms: the first is the standard geometric interferometer delay representing the difference in arrival times at the two antennas for a wavefront from the quasar, while the second is the one-way propagation delay between the TDRSE antenna, where the wavefront is observed, and the White Sands ground station, where the signal is recorded and time-tagged.

For ground-based VLBI, the phase model is simply the delay model multiplied by the observation frequency. Due to the K-band communication links between TDRSE and White Sands, however, the situation is more complicated for this experiment. The phase model takes the form:

$$\phi = \frac{[\vec{r}_{\mathrm{USUDA}} - \vec{r}_{\mathrm{TDRSE}}] \cdot \hat{\epsilon}_{\mathrm{QSO}}}{c} \nu^{\mathrm{QSO}}_{\mathrm{obs}}(S)$$

$$+ \frac{\|\vec{r}_{\mathrm{WS}} - \vec{r}_{\mathrm{TDRSE}}\|}{c} \left(2\nu^{\mathrm{QSO}}_{\mathrm{down}}(K) - \nu^{\mathrm{QSO}}_{\mathrm{obs}}(S)\right)$$

where $\nu^{\mathrm{QSO}}_{\mathrm{obs}}(S)$ is the 2.3 GHz quasar observation frequency and $\nu^{\mathrm{QSO}}_{\mathrm{down}}(K)$ is the 14 GHz downlink frequency for the quasar data. Again the model is the sum of two terms: a geometric interferometer phase and a link term. The first term, representing the geometric phase, is indeed simply the interferometer delay multiplied by the 2.3 GHz S-band observation frequency. The link term, however, consists of the one-way link delay scaled by a frequency of roughly twice the K-band downlink frequency of 14 GHz. The exact value of the frequency factor can be understood as follows: The uplink pilot tone is used to generate a local oscillator frequency onboard the spacecraft of $\nu^{\mathrm{QSO}}_{\mathrm{down}}(K) - \nu^{\mathrm{QSO}}_{\mathrm{obs}}(S)$, which is subsequently used to frequency translate the observed quasar signal to the downlink frequency $\nu^{\mathrm{QSO}}_{\mathrm{down}}(K)$. Any delay errors on the uplink will therefore affect the phase at the effective frequency of $\nu^{\mathrm{QSO}}_{\mathrm{down}}(K) - \nu^{\mathrm{QSO}}_{\mathrm{obs}}(S)$. The relevant frequency for the downlink is $\nu^{\mathrm{QSO}}_{\mathrm{down}}(K)$, and so the total effective frequency for the TDRSE link is $2\nu^{\mathrm{QSO}}_{\mathrm{down}}(K) - \nu^{\mathrm{QSO}}_{\mathrm{obs}}(S)$. Because of this very high effective frequency (of order 25 GHz), the link term for the model phase is more sensitive to spacecraft position errors than the geometric term.

The phase of the White Sands beacon signal provides a highly accurate measurement of the link term. The round trip phase for the beacon signal is

$$\phi_{\mathrm{beacon}} = \frac{\|\vec{r}_{\mathrm{TDRSE}} - \vec{r}_{\mathrm{WS}}\|}{c} \left(2\nu^{\mathrm{beacon}}_{\mathrm{down}}(K)\right)$$

where $\nu^{\mathrm{beacon}}_{\mathrm{down}}(K)$ is the 14 GHz downlink frequency for the beacon data. As the accuracy requirements for the delay model are not stringent, BRTS data were used to calculate the entire delay model. The BRTS data were also used to calculate the geometric term in the phase model, since a full three dimensional TDRSE position vector is required. The beacon data, however, were used to calibrate the link term in the phase model. Details of how the individual corrections were applied at the correlator are described in Section IV.

In addition to accounting for the effects of spacecraft motion, the beacon calibration also removes any effect of the troposphere on the link, since both error sources have the same signature in the link phase. In fact, any non-dispersive error source which corrupts the link will be completely eliminated by the beacon calibration. Finally, spacecraft instrumental phase instabilities common to both channels are largely removed.

E. Calibration of the White Sands Cesium Standard

A hydrogen maser was used as a frequency reference for the Mark III terminal at White Sands. All of the TDRSS local oscillators, however, were by necessity referenced to the TDRSS cesium standard. By calibrating this cesium standard against the hydrogen maser, it was possible to remove the effects of the cesium instability. A comb generator was used to generate a 370 MHz harmonic of the cesium 5 MHz reference. This tone was then mixed down to baseband (0-2 MHz) with a local oscillator derived from the hydrogen maser, and tracked in realtime with a special purpose tone tracker (also referenced to the hydrogen maser) which extracted residual phases at 2 s intervals for the tracked tone. These residuals were used during fringe fitting at the Haystack Observatory correlator in order to correct for the instabilities of the TDRSS cesium.

IV. Data Correlation Procedure

With VLBI data on baselines between earth telescopes, the correlator delay and phase models are fairly simple. The total delay is the geometric delay – the difference in arrival time at the two antennas. The phase is the product of this delay and the sky (observing) frequency. The delay and phase at any epoch can be calculated from only a few parameters: the three

components of the vector baseline in an earth-fixed frame, the longitude of the baseline, and the radio source hour angle and declination. The time variation of delay and phase is given by the rotation of the earth (uniform solid-body rotation is a sufficiently accurate approximation for correlation). Various additional corrections are needed for astrometric or geodetic measurements, but not for measurements of correlated fluxes.

Data from this experiment were correlated with the Haystack Observatory Mk IIIA correlator. The delay and phase models were entered in several stages. The first order models were derived from a constant (earth-fixed) position for the spacecraft (TDRSE is in geosynchronous orbit). This position was obtained from the spacecraft ephemeris, using an epoch near the middle of the observation to be correlated. The approximate geometric delay and phase from the first order models were obtained in the same manner as for two earth-based antennas.

During correlation, the second-order models were applied. Correction polynomials in delay and phase supplied the remainder of the information from the orbit ephemeris (i.e., that not present in the first-order model). These polynomials corrected the geometric delay and phase, and specified the link delay, to acceptable accuracy.

Third order corrections were applied during fringe-fitting. A table of phase residuals was provided, one value for each 2 s correlator output record. The correlated data were rotated by these residuals before being Fourier-transformed. The phase residuals applied in this process arose from measurements made at White Sands (see Sections IIID and IIIE). There were two distinct terms contributing to these residuals. The first was the sum of the high frequency terms in the link phase measurements (i.e., the residuals remaining after a cubic polynomial fit). The second contribution was the measured phase difference between the hydrogen maser and the cesium frequency standard at White Sands.

V. Results

A. Coherence Measurements

Coherence measurements derived from the correlated data are shown in Fig. 4. The lowest curve (A) is the coherence achieved without applying phase residuals (the third-order correction described above) during fringe-fitting. The middle curve (B) shows the improvement that is achieved when the measured phase differences between the cesium and hydrogen maser frequency standards are applied. As the figure shows, the improvement is small at short time scales and large at long time scales. This is consistent with experience with cesium standards in VLBI experiments – good coherence for short time scales and poor coherence at long time scales. The upper curve (C) shows the coherence when the phase residuals for both the link calibration and frequency standards are applied. The link calibration corrects most of the short-term coherence loss. It is unclear why this loss occurred. It may be due to physical motion of the spacecraft, with amplitudes of a few mm and time scales of 10–100 s. Alternatively, it may be due to instabilities in the spacecraft electronics which are common to the two channels (quasar and beacon).

When all corrections were applied, the coherence was 92% at 300 s and 84% at 700 s (Fig. 4, curve C). If the beacon phase is not used, and instead the BRTS ephemeris is used to calibrate the link phase, the coherence falls to 84% at 300 s and 78% at 700 s (Fig. 4, curve B). Finally, if the phase residuals for the cesium clock also are not used (Fig. 4, curve A), the coherence drops to 73% at 300 s and 60% at 700 s. Given that the high link frequency was more important than the observing frequency in limiting the coherence, and given the fact that TDRSE was not designed for VLBI, it is likely that the coherence would be nearly as good (or perhaps better) for a dedicated VLBI observatory observing at frequencies as high as 20–30 GHz.

B. Astronomical Results

The telescopes in Australia and Japan were calibrated in the normal way. A noise diode was used to monitor the system temperature, and observations of sources with known flux were used to measure antenna gain. The TDRSE spacecraft was equipped with an automatic gain control, so that a different calibration method was used, as described in Ref. 5. The basic procedure involved the knowledge that the projected baseline between TDRSE and Australia was sometimes similar to projected baselines on ground baselines at other times. Because the correlated flux on these baselines was known from the calibration of the ground antennas, the sensitivity of TDRSE could be determined. The result was that TDRSE was determined to have an aperture efficiency of 0.4 and a system temperature of 320 K. By comparison, the ratio of gain to system temperature for the 64 m ground antennas was 4,000–5,000 times that for TDRSE.

Correlated flux was detected on a total of six scans for three sources: 1510-089, NRAO 530 (1730-130), and 1741-038, all quasars. All scans for which correlated flux was not detected were known to have had equipment setup or antenna pointing errors. In other words, none of the nondetections were due to inadequate correlated flux on long projected baselines. The maximum baseline was 1.4 earth diameters, on NRAO 530, with baselines longer than one earth diameter obtained for all three sources. The sampling of projected baselines in the u-v plane for NRAO 530, the source for which

the most data were obtained, is shown in Fig. 5. Here, u is the east-west component of the baseline, while v is the north-south component. The track at $v = 1.1 \times 10^8\lambda$ was generated by the TDRSE-Japan baseline, and the track at $v = 5.5 \times 10^7\lambda$ was generated by the TDRSE-Australia baseline. The point at $u = 10^7$, $v = 5.5 \times 10^7\lambda$ was generated by the Japan-Australia baseline. The u-v coverage shown in Fig. 5 is too poor to make a map of a radio source.

Fringe visibilities on the maximum projected baselines were 0.15 (1510-089), 0.05 (NRAO 530), and 0.50 (1741-038). A plot of the correlated flux as a function of projected baseline length is shown in Fig. 6 for 1510-089 and NRAO 530, the two sources with the most data. The correlated flux density drops rapidly with increasing baseline length for NRAO 530, but appears to flatten at 0.3 Jy, implying a brightness temperature of $\approx 4 \times 10^{11}$ K. The correlated flux of 1510-089 drops off more slowly with baseline length. For both sources, even longer baselines are needed to resolve the innermost structure.

VI. Summary

The coherence results described in this article demonstrate the feasibility of transferring a coherent frequency reference to an orbiting satellite with sufficient stability to perform VLBI using a telescope in earth orbit. Careful calibration of the spacecraft communications link is required to achieve the highest coherence. It has also been shown that quasars still contain significant amounts of compact flux on baselines longer than an earth diameter. Togther, these two results demonstrate the technical and scientific feasibility of doing VLBI using a dedicated radio telescope in earth orbit.

A second set of VLBI observations involving the TDRSE satellite is scheduled for January 1987. One of the goals of those observations will be to better understand the limiting error sources after all calibrations have been applied. Debugging of the pointing software for the spacecraft antennas has been accomplished, so the larger pointing window described in Section II will be usable. The increased flexibility in pointing will be used to observe sources at more southerly declinations and at greater eastern and western elongations than was possible in the first experiment. Such observations will achieve projected baselines of 2-2.5 earth diameters (25,000-30,000 km) on some radio sources. Such baselines will extend the investigations of source structure further beyond the limits imposed by the earth's physical size and will provide a probe of very compact radio emission and high brightness temperatures.

Acknowledgments

The TDRSS OVLBI project was ably led by G. Levy, who coordinated manpower and equipment resources worldwide. C. Ottenhoff, S. Di Nardo, C. Christensen, and R. Stavert all played an important role in the design and realization of the calibrations at White Sands. The helpful efforts of the staff at the White Sands Ground Terminal are gratefully acknowledged. F. Jordan provided invaluable support at JPL. M. Maher and K. Blaney provided help in working with the TDRSS organization and in understanding the spacecraft. L. Skjerve, D. Jauncey, and W. Peters set up and ran the VLBI equipment in Australia. A. Whitney, R. Cappallo, and A. Rogers made necessary modifications to the Haystack Observatory Mk IIIA correlator software, and provided much useful advice during fringe-searching. The staffs of ISAS, RRL, and the Nobeyama Radio Observatory were responsible for the data acquisition in Japan. The National Radio Astronomy Observatory contributed by lending equipment that was used at White Sands.

References

1. European Space Agency, "Quasat – a VLBI observatory in space," Proceedings of a Workshop held at Gross Enzersdorf, Austria, 18-22 June 1984.

2. Jordan, J. F., "Quasat – U.S. Status Report," in *Proceedings of the Green Bank Workshop on Radio Astronomy from Space*, National Radio Astronomy Observatory, Green Bank, West Virginia, September 30-October 2, 1986, in press.

3. Schilizzi, R. T., "The U.S.S.R. RadioAstron Space VLBI Project," in *Proceedings of the Green Bank Workshop on Radio Astronomy from Space*, National Radio Astronomy Observatory, Green Bank, West Virginia, September 30-October 2, 1986, in press.

4. Levy, G. S., Christensen, C. S., Jordan, J. F., Preston, R. A., and Burke, B. F., "Orbiting Very Long Baseline Interferometer Demonstration using the Tracking and Data Relay Satellite System," in *Proceedings of International Astronomical Union Symposium No. 110, VLBI and Compact Radio Sources*, Bologna, Italy, June 27-July 1, 1983, edited by R. Fanti, K. Kellermann, and G. Setti, pp. 405-406.

5. Levy, G. S., Linfield, R. P., Ulvestad, J. S., Edwards, C. D., Jordan, J. F., Di Nardo, S. J., Christensen, C. S., Preston, R. A., Skjerve, L. J., Stavert, L. R., Burke, B. F., Whitney, A. R., Cappallo, R. J., Rogers, A. E. E., Blaney, K. B., Maher, M. J., Ottenhoff, C. H., Jauncey, D. L., Peters, W. L., Nishimura, T., Hayashi, T., Takano, T., Yamada, T., Hirabayashi, H., Morimoto, M., Inoue, M., Shiomi, T., Kawaguchi, N., and Kunimori, H., "Very Long Baseline Interferometric Observations Made with an Orbiting Radio Telescope," *Science*, Vol. 234, pp. 187-189, October 10, 1986.

6. Rogers, A. E. E., Cappallo, R. J., Hinteregger, H. F., Levine, J. I., Nesman, E. F., Webber, J. C., Whitney, A. R., Clark, T. A., Ma, C., Ryan, J., Corey, B. E., Counselman, C. C., Herring, T. A., Shapiro, I. I., Knight, C. A., Shaffer, D. B., Vandenberg, N. R., Lacasse, R., Mauzy, R., Rayhrer, B., Schupler, B. R., and Pigg, J. C., "Very-Long-Baseline Radio Interferometry: The Mark III System for Geodesy, Astrometry, and Aperture Synthesis," *Science*, Vol. 219, pp. 51-54, January 7, 1983.

7. Rogers, A. E. E., and Moran, J. M., "Coherence Limits for very long baseline interferometry," *IEEE Transactions on Instrumental Measurements*, Vol. IM-30, No. 4, pp. 283-286, 1981.

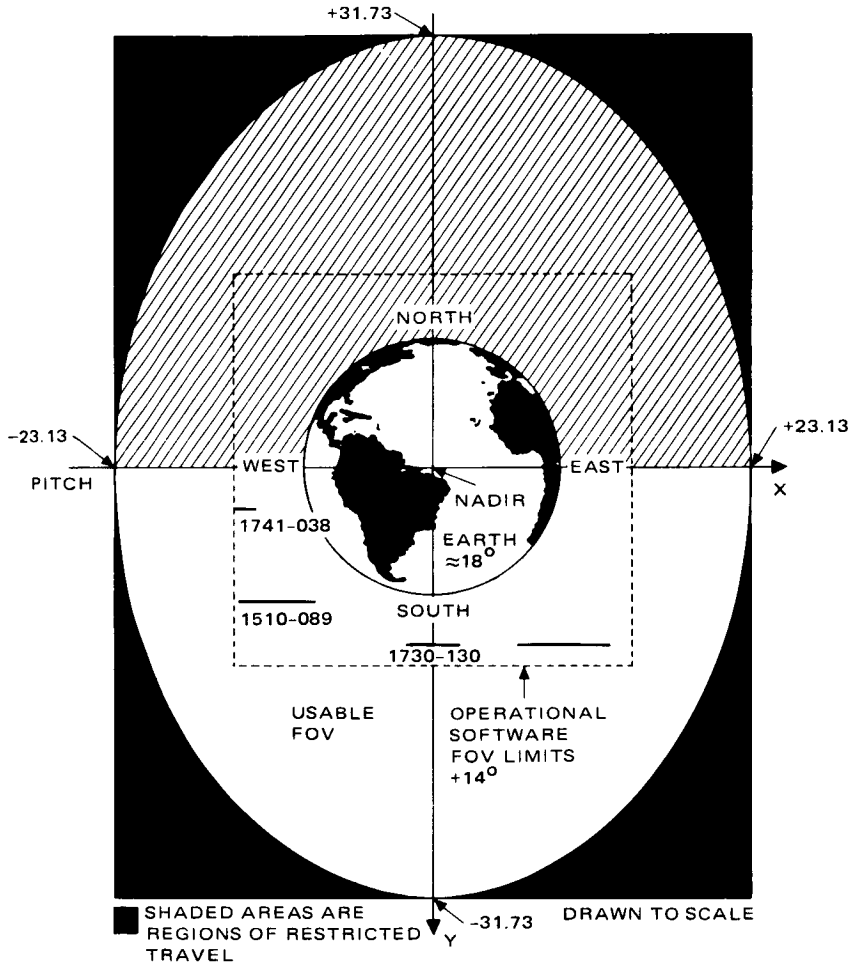

Fig. 1. Field of view of the TDRSE antenna. The large ellipse is the large pointing window specified for the antenna, while the smaller square is the field-of-view (FOV) normally allowed by the operational software. Observations in the hatched region were not allowed. Approximate locations of the radio sources successfully observed are indicated.

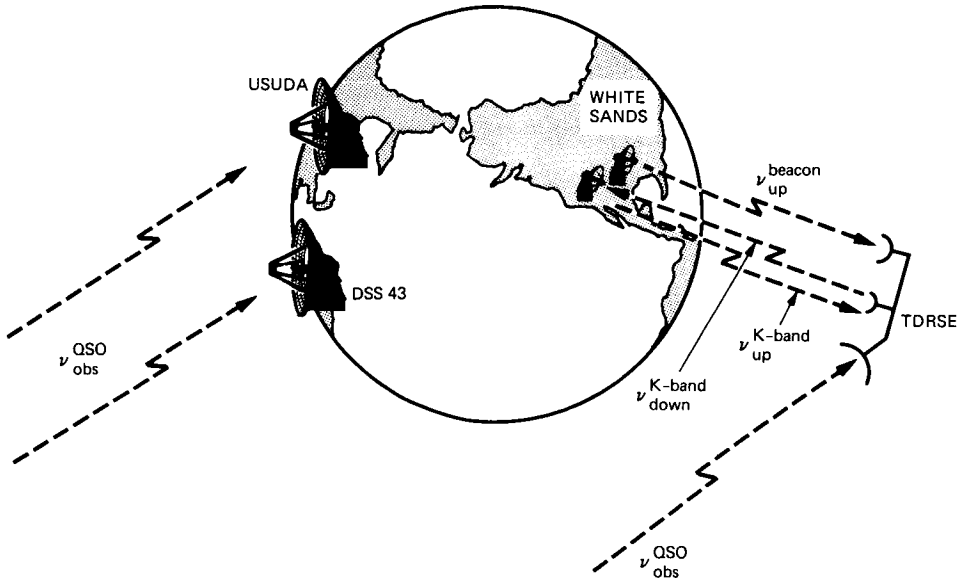

Fig. 2. Link configuration for the TDRSS OVLBI observations

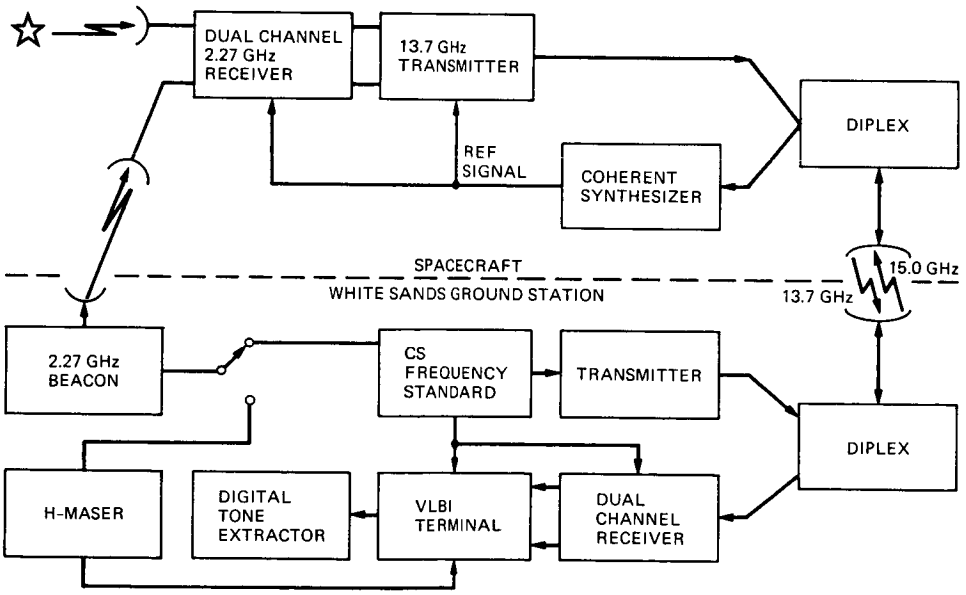

Fig. 3. Simplified block diagram of the configuration used for VLBI obserevations made with the TDRSE spacecraft

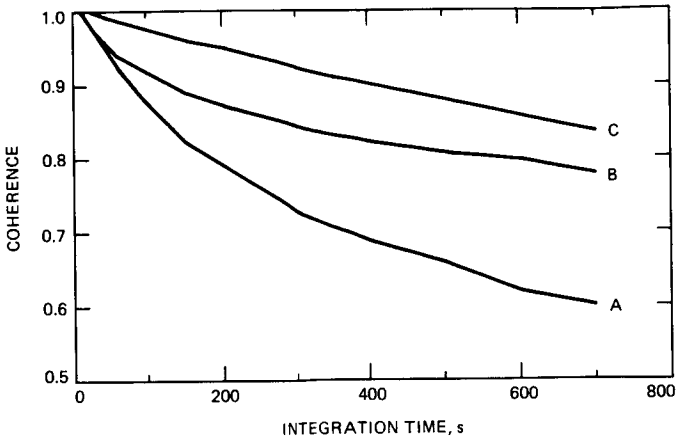

Fig. 4. TDRSS OVLBI coherence results for three different cases. Corrections included in generating curves A, B, and C are described in text.

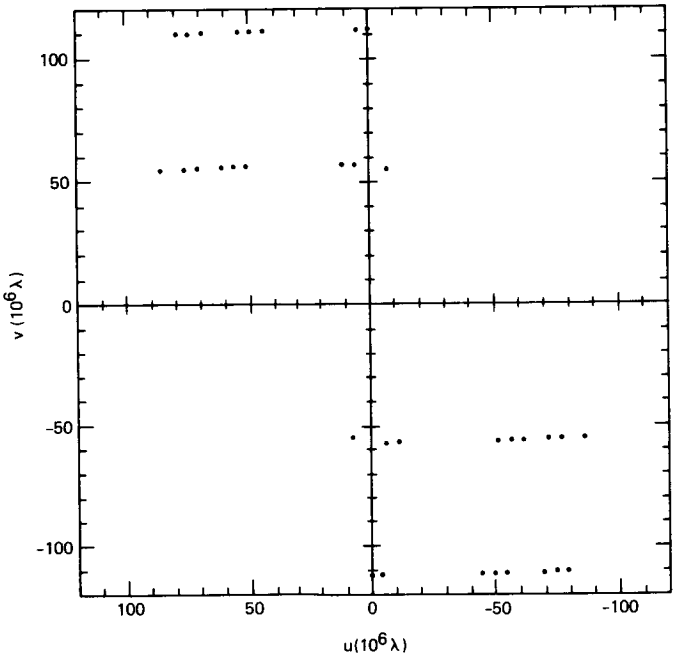

Fig. 5. Coverage of the u–v plane for the observations of NRAO 530. The east–west projection is specified by u and the north–south projection is given by v, both in units of millions of S-band wavelengths.

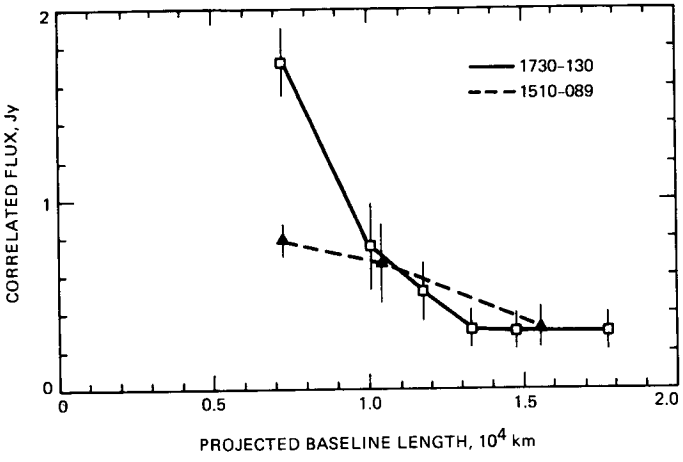

Fig. 6. Plots of correlated flux versus projected baseline length ("visibility plots") for observations of two quasars, as found in the TDRSS OVLBI experiment. The earth diameter is approximately 1.3×10^4 km.